

Retro-reflective Beamforming Technique with Applications in Wireless Power Transmission

WANG Xin^{1*}, LU Mingyu²

1. College of Electronic and Information Engineering, Nanjing University of Aeronautics and Astronautics, Nanjing 211106, P.R. China;

2. Department of Electrical and Computer Engineering, West Virginia University Institute of Technology, West Virginia 25801, USA

(Received 5 July 2019; revised 25 July 2019; accepted 30 July 2019)

Abstract: Retro-reflective beamforming technique has the potential of enabling efficient wireless power transmission over long distance (on the order of meters and even kilometers). In retro-reflective beamforming, wireless power transmission is guided by pilot signal: Based upon pilot signal broadcasted by a wireless power receiver, a wireless power transmitter delivers focused microwave power beam(s) onto the location of wireless power receiver. When the wireless power receiver's location is not fixed or when the wireless power receiver's location is unknown to the wireless power transmitter, the microwave power beam would follow the wireless power receiver's location dynamically as long as the wireless power receiver broadcasts pilot signal periodically. This paper reviews our research endeavors in recent years on retro-reflective beamforming technique targeting three applications: (1) wireless charging for low-power mobile/portable electronic devices, (2) space solar power satellites (SSPS) application, and (3) wireless charging in fully-enclosed space. The feasibility and potential of retro-reflective beamforming technique with applications in wireless power transmission are demonstrated by some preliminary experimental results.

Key words: wireless power transmission; retro-reflective beamforming; microwave; antenna array; pilot signal

CLC number: TN99 **Document code:** A **Article ID:** 1005-1120(2019)04-0545-21

0 Introduction

Wireless power transmission, i. e., delivering electrical power without using wires/cables, implies numerous appealing applications. The best-known wireless power transmission technique is inductive coupling^[1]; for instance, commercially-available wireless charging pads for cell phones are based on inductive coupling technique. As the inductive coupling technique takes advantage of non-propagating magnetic field, wireless power transmission based on inductive coupling is limited to short distance (on the order of centimeters, typically). Employing propagating electromagnetic waves in the radio frequency (RF) or microwave frequency range as the carrier of wireless power has been demonstrated ca-

pable of reaching long distance (on the order of meters and even kilometers)^[2]. Meanwhile, optical power transmission (that is, employing optical waves as the carrier of wireless power) is also capable of reaching long distance^[3-4]. Relative to optical power transmission, RF/microwave power transmission enjoys several advantages. First, RF/microwave has better penetration capability than optical waves. Second, conversion efficiency between DC power and microwave power is usually higher than that between DC power and optical power. Third, microwave beams can be steered straightforwardly via phase control, whereas beam steering without resorting to mechanical motion is much more difficult in the optical regime. Thus, RF/microwave power transmission is an excellent candidate when the dis-

*Corresponding author, E-mail address: wang90@nuaa.edu.cn.

How to cite this article: WANG Xin, LU Mingyu. Retro-reflective Beamforming Technique with Applications in Wireless Power Transmission[J]. Transactions of Nanjing University of Aeronautics and Astronautics, 2019, 36(4): 545-565.

<http://dx.doi.org/10.16356/j.1005-1120.2019.04.002>

tance between wireless power transmitter and wireless power receiver is beyond the order of centimeter and when the spatial relationship between wireless power transmitter and wireless power receiver is not fixed.

As a far-from-complete review of the history of RF/microwave power transmission, several historical experiments are highlighted below. In 1960s, Brown demonstrated supplying microwave power from a ground station to a helicopter, which is probably the first impactful and well-documented demonstration of RF/microwave power transmission in the history^[5]. In an experiment carried out by NASA JPL in 1975, 30 kW of RF power was successfully delivered over one mile, i.e., 1.6 km^[6-7]. The Stationary High Altitude Relay Program (SHARP) initiated in Canada in 1980s aims to provide microwave power to small aircrafts^[8]. A program similar to SHARP, named MIcrowave Lifted Airplane eXperiment (MILAX), was active in Japan in 1990s^[9]. In 1993, International Space Year-Microwave Energy Transmission (ISY-METS) experiments were conducted in Japan to achieve microwave power transmission between spacecrafts^[10]. A case study from 1997 to 2004 is reported in Ref. [11] to construct point-to-point wireless electricity transmission to a small isolated village called Grand-Bassin in France. In 2009, the feasibility of using a car-borne power broadcaster to power sensors installed over a bridge is studied in Ref. [12].

Since 2013, a range of research efforts on microwave power transmission are conducted collaboratively between Nanjing University of Aeronautics and Astronautics and West Virginia University^[13]. Specifically, the collaborative research focuses on retro-reflective beamforming technique, as depicted

by Fig. 1. The wireless power transmitter includes an array of antenna elements. A wireless power receiver receives wireless power from the wireless power transmitter via the following two steps:

(1) The wireless power receiver broadcasts pilot signal, which is a low-power signal.

(2) In response to the pilot signal, the wireless power transmitter constructs focused microwave power beam onto the location of wireless power receiver.

When the wireless power receiver is in motion, the microwave power beam would follow the wireless power receiver's location dynamically as long as the wireless power receiver broadcasts pilot signal periodically.

The underlying theory of retro-reflective beamforming is "time-reversal", which takes advantage of channel reciprocity to accomplish a space-time matched filter^[14]. Specifically, the propagation of pilot signal follows "the channel from wireless power receiver to wireless power transmitter", whereas the propagation of microwave power follows "the channel from wireless power transmitter to wireless power receiver". If these two channels are reciprocal to each other and if the microwave power transmission is tailored to be the retro-reflected version of pilot signal, microwave power is spatially focused onto the location from which the pilot signal stems, that is, the location of the wireless power receiver. Furthermore, spatial focusing due to retro-reflection/time-reversal does not suffer from multi-path in environments^[15-16]. As another magnificent advantage of retro-reflective beamforming technique, re-configuration of microwave power transmission could be accomplished electronically, i.e., without resorting to mechanical control.

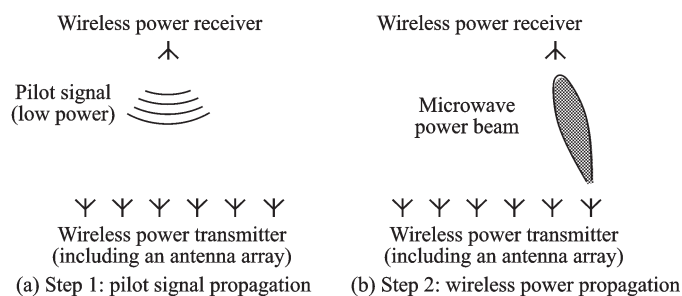


Fig.1 Depiction of retro-reflective beamforming technique for wireless power transmission

Retro-reflective beamforming technique has been researched for years^[17-19], with widespread applications including wireless communication, radar, and wireless power transmission. It is worthwhile noting that, retro-reflective beamforming in the context of wireless power transmission application has two unique technical concerns compared with wireless communication and radar applications. First, the wireless power transmission application aims at maximal power transmission efficiency. Typically in order to achieve high power transmission efficiency, the transmitter and/or the receiver must employ antennas with large aperture. When the antenna dimension is large with respect to the transmitter-receiver distance, the far-zone condition (that is, $d > 2D^2/\lambda$, where d is the distance between transmitter and receiver, D the antenna dimension, and λ the wavelength) would not be satisfied. As a result, the transmitter and receiver stay in each other's near-zone rather than far-zone in a typical wireless power transmission application. Second, in the wireless power transmission application the power level associated with wireless power propagation (Fig. 1 (b)) is much higher than the power level associated with pilot signal propagation (Fig. 1 (a)). Consequently, it is vital to isolate pilot signal propagation from wireless power propagation, because the wireless power propagation is considered as an interference/jammer by the receiver of pilot signal.

Fig. 2 illustrates an implementation scheme of retro-reflective beamforming, with the assumption that the transmitter and receiver are in each other's far-zone, in other words, with the assumption that $d > 2D^2/\lambda$ is satisfied. Also, the antenna elements in the wireless power transmitter are assumed to be

equi-spaced along one dimension in space. In the first step of retro-reflective beamforming (Fig. 2 (a)), the wireless power receiver broadcasts a continuous-wave pilot signal. Since the wireless power receiver resides in the far-zone of wireless power transmitter, pilot signal reaches the wireless power transmitter as a plane wave with planar equi-phase surfaces, as depicted in Fig.2(a). As a result, the phases detected by the array's elements exhibit a linear pattern. In the second step of retro-reflective beamforming (Fig.2(b)), the wireless power transmitter transmits wireless power, which is a continuous-wave with the same frequency as pilot signal's (but of higher power level), to the wireless power receiver. Each antenna element is excited with phase negative to the phase of pilot signal received in the first step, as shown in Fig. 2 (b). In other words, the phase profile of wireless power transmission in the second step is conjugate to the phase profile of pilot signal reception in the first step. According to the theory of phased array, the wireless power transmitter generates a plane wave with propagation direction opposite to the pilot signal's incoming direction. The scheme illustrated in Fig.2 is termed "retro-directive beamforming" in many literatures, since pilot signal propagation and wireless power propagation both exhibit explicit propagation directions. As a matter of fact, retro-directive beamforming is a special case of retro-reflective beamforming when the wireless power receiver resides in the far-zone of wireless power transmitter.

If a wireless power receiver does not reside in the far-zone of wireless power transmitter, the implementation scheme of retro-reflective beamforming is essentially the same as Fig.2, but with some

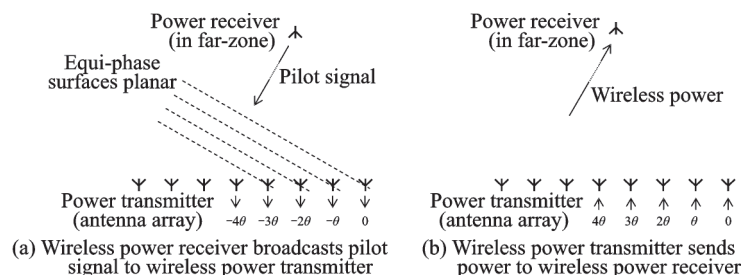


Fig.2 An implementation scheme of retro-reflective beamforming when a wireless power receiver resides in the far-zone of wireless power transmitter

slight and interesting differences, as illustrated in Fig.3. In the first step, the pilot signal does not behave as a plane wave when it reaches the wireless power transmitter; rather, its equi-phase surfaces are curved, as displayed by Fig.3(a). Consequently, the phase profile of pilot signal received by the antenna elements does not exhibit linear pattern. When the phase received by the right-most element is defined to be zero, the phase received by an element in the middle is denoted as $-\theta$; apparently, phase $-\theta$ corresponds to the extra path specified by a piece of thick line segment in Fig. 3 (a). If the right-most element is excited with phase zero and the middle element is excited with phase θ in the sec-

ond step (Fig.3(b)), their radiations reach the wireless power receiver with the same phase, in other words, their radiations are constructive at the wireless power receiver. The above analysis holds true for every element of the array. Therefore, exciting the array elements with phase profile conjugate to the pilot signal's phase profile leads to focusing wireless power onto the wireless power receiver's location. When the wireless power receiver moves further and further away from the wireless power transmitter, the scenario in Fig.3 evolves to Fig.2. Thus, Fig.2 is a special case of Fig.3, and Fig.3 embodies a general scheme of retro-reflective beamforming technique.

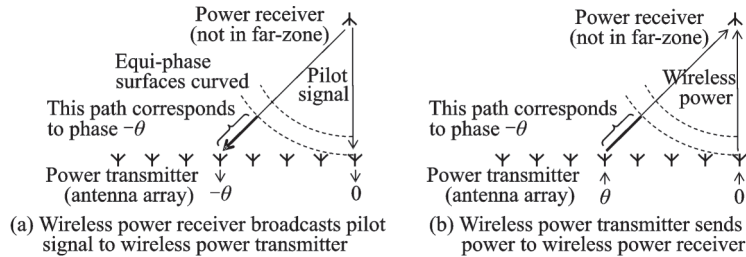


Fig.3 An implementation scheme of retro-reflective beamforming when a wireless power receiver resides in the near-zone of wireless power transmitter

Figs.2 and 3 jointly explain the relationship between “retro-reflective beamforming” and “retro-directive beamforming”. Specifically, “retro-directive beamforming” is a special case of “retro-reflective beamforming” when the wireless power receiver resides in the far-zone of wireless power transmitter, whereas “retro-reflective beamforming” is applicable in both far-zone and near-zone scenarios^[20]. In a typical wireless power transmission application, the transmitter and receiver do not stay in each other's far-zone, as discussed earlier in this section. Hence in our endeavors, “retro-reflective beamforming” is used as the name of the technique we pursue to accomplish efficient wireless power transmission, albeit “retro-directive beamforming” is adopted in literatures more popularly.

Numerous technical approaches have been proposed to implement the retro-reflective beamforming schemes illustrated in Fig.2 or Fig.3, such as Van Atta method^[21], heterodyne method^[22], and methods based on phase-lock loop^[23]. Nevertheless,

some of these methods cannot be applied to wireless power transmission applications directly. For example in wireless power transmission applications, it is vital to prevent wireless power from jamming the receiver of pilot signal; and thus if a method does not offer sufficient isolation between wireless power and pilot signal, it would not be a good option for wireless power transmission applications. Moreover in practice, various wireless power transmission applications are drastically different from one another (three of them are elucidated in this paper). It is almost impossible for one technical approach to fit all the applications. During the past few years, we conducted a range of research on retro-reflective beamforming targeting three specific wireless power transmission applications: (1) wireless charging for low-power mobile/portable electronic devices, (2) space solar power satellites (SSPS) application, and (3) wireless charging in fully-enclosed space. Our research efforts and findings for these three applications are presented in Sections 1, 2, and 3, re-

spectively. The last section of this paper, Section 4, relates to our conclusions regarding retro-reflective beamforming technique with applications in wireless power transmission.

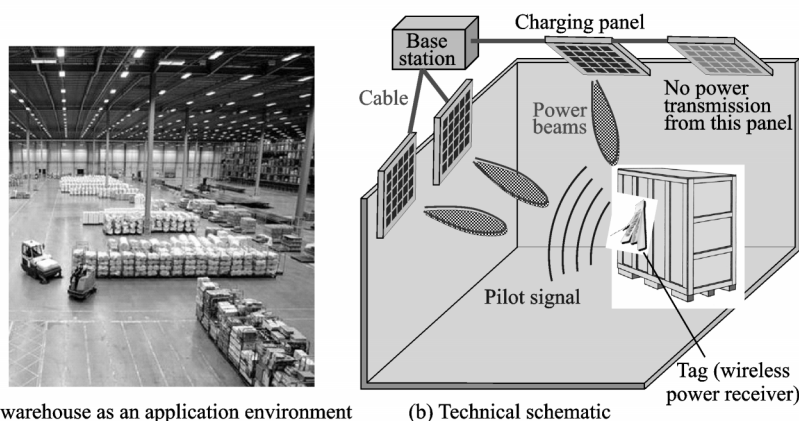
1 Retro-reflective Beamforming Technique for Charging Low-Power Mobile/Portable Electronic Devices Wirelessly

Numerous portable electronic devices, such as laptops, cell phones, digital cameras, and electric shavers, rely on rechargeable batteries and must be routinely charged by the line power. A wireless charging technique capable of delivering electrical power to these portable devices would make them tether free and “truly portable”. Nevertheless, a range of established regulations imposes restrictions on the power level associated with wireless transmission, for the purpose of electromagnetic compatibility and human safety^[24-26]. Compliance with these regulations makes it a challenging task to deliver wireless power of a few Watts or higher remotely. Remote delivery of wireless power on the order of milli-Watt, though not sounding extremely exciting, is still useful in practice. In fact, a large number of low-power electronic devices like radio frequency identification tags and wireless sensors may benefit from wireless power transmission, particularly in scenarios where wired charging is intractable (for examples, when tags are unattended and when sensors are buried underneath the ground)^[27].

In Fig.4(a), a warehouse is used as an example of practical environments in which “wireless charging for low-power mobile/portable electronic devices” could find applications. Suppose there are thousands of containers in the warehouse, and each container has one radio frequency identification tag attached to it. Fig.4(b) depicts a retro-reflective beamforming scheme to deliver wireless power to the tags. The wireless power transmitter consists of a base station and multiple charging panels. The charging panels are mounted over the ceiling or walls. The base station and charging panels are connected to each other through cables. Tags in the warehouse receive wireless power from the wireless power transmitter via the following two steps: (1) One or more than one tag(s) broadcast pilot signals; (2) In response to the pilot signals, the charging panels jointly construct focused microwave power beam(s) onto the target tag(s).

A charging panel transmits power only if it has line-of-sight interaction with the target tag. If the line-of-sight path is blocked by any obstacle, the charging panel is deactivated such that the obstacle, which might be human being, is not illuminated by power beams directly^[28].

Timing sequence of the retro-reflective beamforming scheme in Fig.4 is depicted by a flow chart in Fig.5. Interactions between the wireless power transmitter and wireless power receiver are toggled among three modes: communication mode, radar mode, and charging mode. The process in Fig.5



(a) A warehouse as an application environment (b) Technical schematic

Fig.4 An example of wireless charging for low-power mobile/portable electronic devices

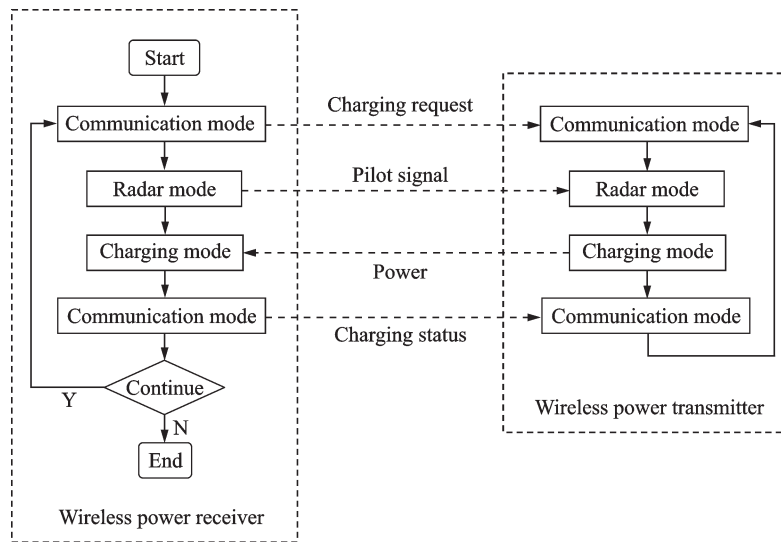


Fig.5 Timing sequence of the retro-reflective beamforming scheme in Fig.4

starts when a wireless power receiver (the tag in Fig.4) communicates a “charging request” signal to the wireless power transmitter. Once the wireless power transmitter acknowledges “charging request”, the system enters radar mode in which the wireless power receiver transmits pilot signal and the wireless power transmitter prepares for beamforming through analyzing the pilot signal. When the wireless power transmitter is ready, both the wireless power transmitter and wireless power receiver march into charging mode and power is delivered to the wireless power receiver through spatially-focused beams. In practice, the environment may change during the charging process; for examples, the wireless power receiver may move and/or another wireless power receiver may request for charging. As a result, the beamforming plan must be adjusted accordingly. To accommodate these situations, the system is periodically switched from charging mode to communication mode and radar mode such that the system would be reconfigured in reaction to the environmental changes. Apparently in Fig.5, “pilot signal propagation” and “wireless power propagation” are isolated from each other in time; in other words, time-division duplexing is employed in Fig.5.

One of the experimental setups for verifying the scheme of Fig.4 is depicted in Fig.6^[29]. The wireless power transmitter includes one charging panel, which further includes four microstrip anten-

na elements. The wireless power receiver has one microstrip antenna. The power transmitter is stationary, whereas the wireless power receiver moves along the x axis in the experiments and it emulates a mobile/portable device. “ $x = 0$ ” denotes the location over the x axis right in front of the charging panel. The distance between “ $x = 0$ ” and the wireless power transmitter is 50 cm.

The experimental procedure associated with Fig.6 has the following two steps:

(1) Power receiver transmits pilot signal to power transmitter (Fig.6(a)). The power receiver’s antenna is connected to a pulse generator. The pulses transmitted by the power receiver’s antenna behave as the pilot signal. In our implementation, the pulses are generated via amplitude-modulating a continuous-wave at 2.08 GHz by periodic square pulses with pulse width of 25 ns and pulse repetition rate of 4 MHz. The pilot signal is received by the four antennas of the power transmitter and then analyzed by the “pilot signal analyzers”.

(2) Power transmitter transmits wireless power to power receiver (Fig.6(b)). In this step, the power transmitter’s four antennas are fed by microwave power generators. The microwave power generators are configured according to the outcome of Step (1) so that a focused power beam is constructed toward the location from which the pilot signal is emitted. Wireless power collected by the power receiver’s antenna is detected by either a power me-

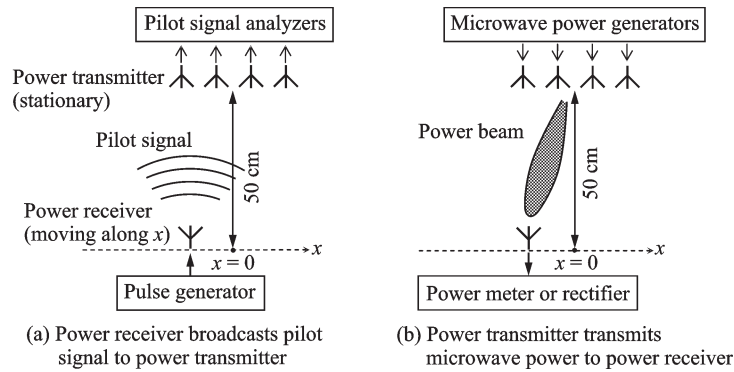


Fig.6 Depiction of an experimental setup with one charging panel

ter or a rectifier.

A photo of the experimental setup in Fig. 6 is shown in Fig. 7. In Step (2), wireless power is delivered from the power transmitter to power receiver and wireless power reception is indicated by a light emitting diode (LED) on the power receiver.

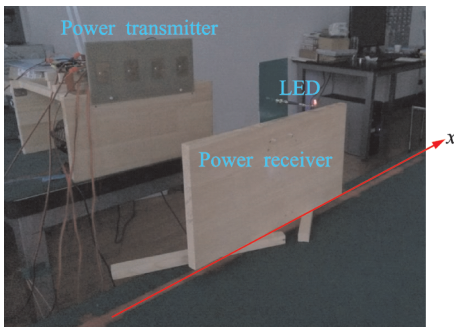


Fig.7 A photo of experimental setup with one charging panel

In the experiments, a pilot signal is broadcasted by the power receiver at a location denoted as x_0 , and the pilot signal is received and analyzed by the power transmitter; then after the power transmitter is configured by the outcome of analyzing the pilot signal, the power receiver moves along x axis to detect the wireless power. In all the experiments, the total power transmitted by the power transmitter is roughly 1 W (that is, 250 mW from each of its four antenna elements). In Fig. 8, microwave power measured by a power meter is plotted when the wireless power is carried by frequency 2.08 GHz. The four subplots in Fig. 8 correspond to " $x_0=0$ " " $x_0=-10$ cm" " $x_0=-20$ cm" and " $x_0=-30$ cm", respectively. The calculated curves in Fig. 8 are obtained using the Friis transmission equation. In Fig. 8, the measured data and calculated data gener-

ally match each other. The measured data in reaction to " $x_0=0$ " has a peak at " $x=0$ " with peak value of the received power of about 14 mW. The measured value (14 mW) is slightly larger than the calculated value (12 mW). We believe it is because the power receiver does not reside in the power transmitter's far-zone, which makes Friis equation not very precise. When x_0 changes to -10 , -20 , and -30 cm, the power beam is steered and the beam center keeps track of x_0 . In our experiments, the beam cannot be steered beyond -30 cm due to the limitation of individual microstrip antennas' radiation patterns. When x_0 takes positive values, the power beam is steered and the beam center tracks x_0 as well; beam steering for positive x_0 values is not demonstrated as it is symmetric to the negative x_0 values.

On the basis of the experimental setup in Fig. 6, another set of experiments are carried out as

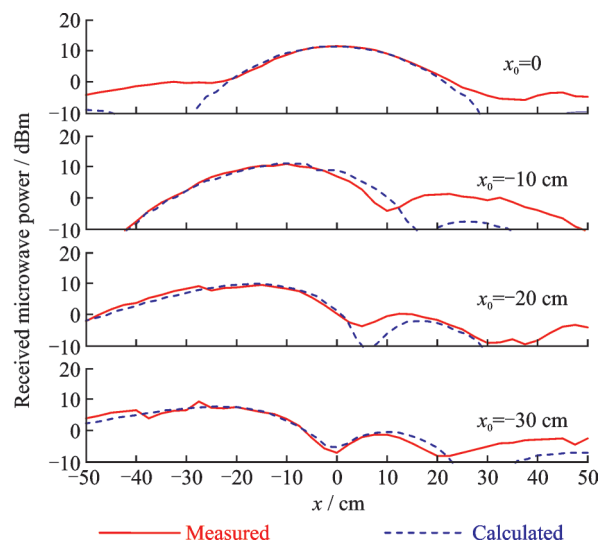


Fig.8 Received microwave power at frequency 2.08 GHz^[29]

illustrated by Fig. 9. As a progress with respect to Fig. 6, the wireless power transmitter in Fig. 9 includes two charging panels, each consisting of four antenna elements^[30]. The two charging panels are placed over x axis and y axis, respectively. The wireless power receiver moves within a certain region in the x - y plane. Fig. 10 shows a photo of the experimental setup corresponding to Fig. 9. The antennas of the wireless power transmitter are microstrip antennas polarized along z direction. The antenna of the wireless power receiver is a monopole antenna, with omni-directional radiation pattern in the x - y plane.

Some results measured with the configuration

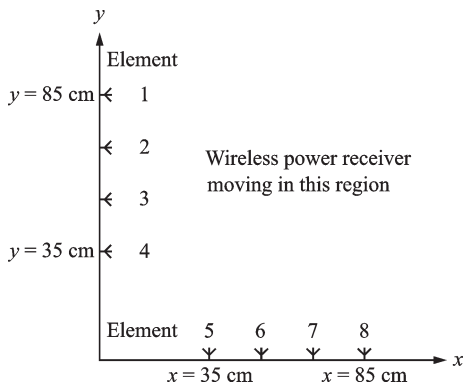


Fig.9 Illustration of an experimental setup with two charging panels

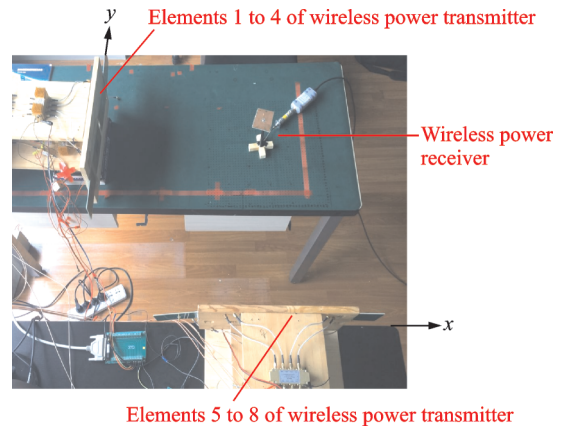


Fig.10 A photo of experimental setup with two charging panels

in Figs. 9, 10 are shown in Fig. 11. The microwave power transmitted by each antenna element of the wireless power transmitter is roughly 175 mW, with a total of $175 \text{ mW} \times 8 = 1.4 \text{ W}$. A power meter is connected to the wireless power receiver's antenna, and the measured microwave power is plotted in Fig. 11. The two plots in Figs. 11(a) and (b) are obtained when the pilot signal is broadcasted from $(x = 60 \text{ cm}, y = 60 \text{ cm})$ and $(x = 70 \text{ cm}, y = 70 \text{ cm})$, respectively. Fig. 11 clearly demonstrates that, the microwave power is focused onto the location from which the pilot signal is broadcasted as a result of retro-reflective beamforming.

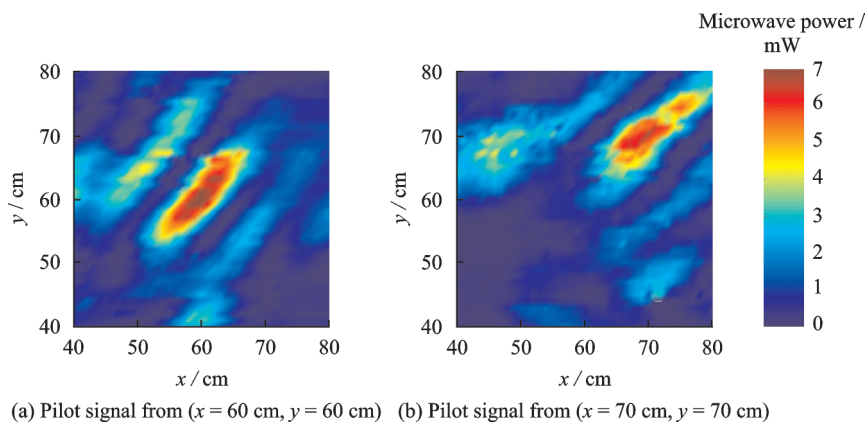


Fig.11 Microwave power distribution measured with the configuration in Figs. 9, 10^[30]

2 Retro-reflective Beamforming Technique for SSPS Application

The concept of SSPS was proposed in 1968, in which solar energy on the order of Giga-Watt is

harvested by satellites over the earth's geostationary orbit and then the harvested energy is delivered to the earth wirelessly^[31]. As an extremely complex system, the feasibility of SSPS is still under assessment/discussion to date.

Ref. [32] provides a comprehensive review of the history of SSPS. Below are several recent developments relevant to SSPS that are not included in Ref. [32]. In 2015, Caltech was awarded a \$17.5 million project by Northrop Grumman Corporation to develop SSPS solutions^[33]. In recent years, two experiments of wireless power transmission were reported by Japanese researchers. Both were carried out on the earth but intended for SSPS applications, one by Japan Aerospace Exploration Agency over 55 m^[34], and the other by Mitsubishi Heavy Industries, Ltd. over 500 m^[35].

Wireless power transmission is a critical ele-

ment of the SSPS concept. The microwave frequency of 5.8 GHz appears a nice candidate to carry the wireless power from satellites to earth, as discussed in Ref. [32]. Moreover, retro-reflective beamforming is believed one of the enabling techniques in order to accomplish efficient, reliable, and safe wireless power transmission from satellites to earth. As illustrated by Fig.12, the retro-reflective beamforming technique in the context of SSPS includes the following two steps: (1) Pilot signal is transmitted from the earth to the satellite; (2) In reaction to the pilot signal, a microwave power beam is constructed from the satellite to the earth.

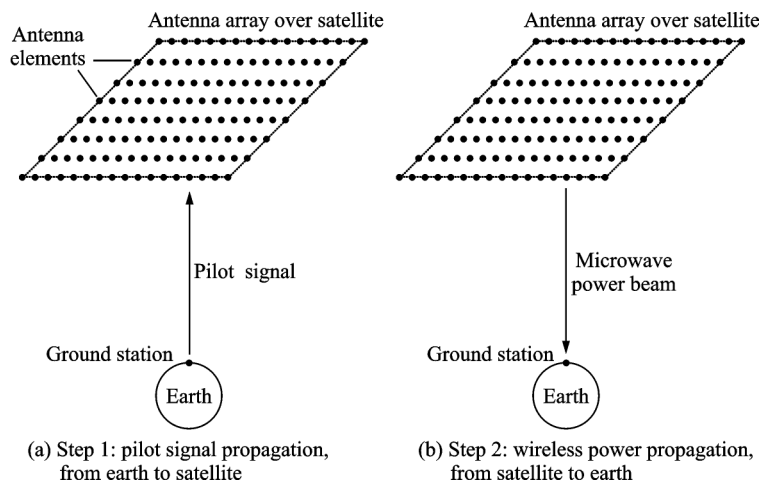


Fig.12 Illustration of retro-reflective beamforming technique in the context of SSPS

With respect to the earth, a satellite is a dynamically-stable platform; in other words, a satellite's physical position and orientation are under constant control in practice. Meanwhile, the power level of wireless power transmission is as high as Giga-Watt in SSPS applications. Due to the two facts above, it is imperative to ensure that most of the wireless power is received by a designated ground station on the earth when the satellite's physical condition is in constant change, as the deviation of wireless power from the designated ground station would result in not only power loss but also possible hazards. The retro-reflective beamforming technique in Fig. 12 is therefore very necessary for the SSPS system; The antenna array over the satellite generates a narrow power beam, and the power beam is steered toward a designated ground station

precisely with the aid of pilot signal.

The two wireless power transmission applications presented in Section 1 and this section respectively, i. e., wireless charging for mobile/portable devices and SSPS, are drastically different from each other in many practical perspectives, as shown in Table 1. "Wireless charging for mobile/portable devices" does not call for long-distance power transmission in practice, typically less than 10 m^[27]. In contrast, the distance between geostationary satellites and earth is as large as 36 000 km in SSPS application. Due to the concerns of electromagnetic compatibility and/or human safety, it is not very probable for a mobile/portable electronic device to receive wireless power beyond milli-Watt level in the everyday life environments. The SSPS application, whereas, intends to supply power on the order

of Giga-Watt to millions of users on the earth. In “wireless charging for mobile/portable devices”, the mobile/portable devices must be tracked over a certain spatial region (a room, for instance) usually, whose size is comparable with the distance of wireless power transmission. In SSPS application, the spatial relationship between wireless power transmitter and wireless power receiver is in constant change as well. However as discussed above, the deviation of microwave power beam from the designated ground station by more than one kilometer is intolerable in practice, and with respect to the 36 000 km distance, 1 km deviation is translated to

small angles of beam-steering. In every wireless power transmission application, it is vital to isolate pilot signal propagation from wireless power transmission. A time-division scheme is proposed for the “wireless charging for mobile/portable devices” application in Section 1. Because the power level associated with SSPS application is as large as Giga-Watt, it would be difficult and awkward (if not impossible) to switch the wireless power on and off periodically in time. As a result, frequency-division is a better approach than time-division in order to separate pilot signal and wireless power in SSPS application^[36].

Table 1 Comparison between two wireless power transmission applications

Property	Wireless charging for mobile/ portable devices	SSPS
Distance of wireless power transmission	< 10 m	≈ 36 000 km
Power level delivered to wireless power receiver	mW	GW
Tracking range with respect to distance	Large	Small
Isolation between pilot signal and wireless power	Time-division	Frequency-division

Suppose a conventional phased array is employed to beam microwave power from a satellite to the earth. The array is comprised of $N_x \times N_z$ antenna elements deployed along x and z directions, as depicted in Fig.13(a). The antenna elements are assumed to be identical to one another and equi-spaced by d_x and d_z along x and z directions, respectively. Further, it is assumed that $d_x = d_z = \lambda_0/2$, where $\lambda_0 = c/f$, c is the speed of light in free space, and $f = 5.8$ GHz is the carrier frequency of microwave power. The radiation pattern of a phased array is the product of individual element's radiation pattern and array factor^[37]. In SSPS application illustrated by Fig.12, the power receiver on earth is far away from the phased array (36 000 km away, to be specific). In order to generate a narrow beam targeted at the power receiver on earth, the phased array must have large aperture. Consequently, the radiation pattern of the phased array is dominated by its array factor. When $N_x = N_z = 39$, the phased array's aperture size in x - z plane is about 1 m by 1 m. Its array factor in x - y plane is plotted in Fig.13(b), when all the elements are fed in phase.

The array factor exhibits a main beam toward $+y$ direction, as expected. The array factor in z - y plane is the same as in x - y plane. The 3 dB beamwidth of the main beam is found to be roughly $2.6^\circ \times 2.6^\circ$. At location $y = y_0 = 36\ 000$ km (that is, over the earth surface), the main beam corresponds to a circular region with diameter of 1 634 km approximately.

A few sets of data with various array aperture dimensions are tabulated in Table 2. With the increase of array aperture, the main beam becomes narrower, and the beamwidth is inversely proportional to the aperture size. When the array aperture size is 1 km by 1 km, the main beam's coverage over earth surface has diameter 1.6 km. The beamwidth in Table 2 is defined by the 3 dB criterion, that is, the power intensity at the beam's rim is half as the power intensity at the beam's center. Consequently, to maintain high power efficiency the power receiver on earth surface ought to be much larger than the region covered by the 3 dB beamwidth. In addition, the analysis above is under idealistic scenario, and in reality it is reasonable to anticipate the beam to be significantly wider. After taking all of

these factors into account, it appears that the array aperture should have size of at least 1 km by 1 km

such that the power receiver over earth is practically-viable.

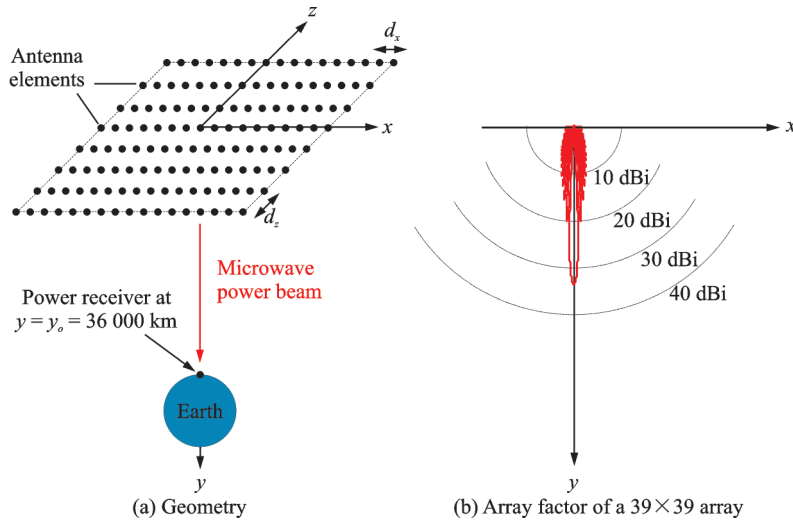


Fig.13 Radiation due to a conventional phased array in SSPS application

Table 2 Physical dimension and beamwidth of conventional phased array in SSPS application

Array aperture	Number of elements	3 dB beamwidth	3 dB beam over earth surface
1 m × 1 m	39 × 39	2.6° × 2.6°	With diameter 1 634 km
10 m × 10 m	387 × 387	0.26° × 0.26°	With diameter 163 km
100 m × 100 m	3 867 × 3 867	0.026° × 0.026°	With diameter 16 km
1 km × 1 km	38 668 × 38 668	0.002 6° × 0.002 6°	With diameter 1.6 km

Assume the antenna array in Fig.13 has aperture dimension 1 km by 1 km, with $N_x = N_z = 38\,668$. Also, assume that the pilot signal is a continuous-wave (CW) signal at 5.8 GHz generated by a point source located at $y = y_0$ (Fig.14(a)). When the pilot signal is received by an antenna element at location $(x, 0, z)$, its phase is recorded as $\varphi(x, z)$. If the phase at the center element is specified as the phase reference (that is, $\varphi = 0$ at $(x=0, z=0)$)

$$\varphi(x, z) = -k_0 \sqrt{(y_0)^2 + x^2 + z^2} + k_0 y_0$$

$$\xrightarrow{(y_0)^2 \gg x^2 + z^2} -k_0 \frac{x^2 + z^2}{2y_0} \quad (1)$$

The distribution of $\varphi(x, z)$ is plotted in Fig.14(b). At the four corners (i. e., when $|x| = 500$ m and $|z| = 500$ m), φ is as large as -48° . It means that, the pilot signal does not behave as a plane wave when it reaches the array aperture; as illustrated in Fig.14(a), the equi-phase surface associated with the pilot signal propagation is curved with respect to the array aperture. In other words, though separated from each other by 36 000 km, the satellite and the

ground station stay in each other's near-zone rather than far-zone^[38]. Obviously, it is because the antenna apertures over satellite and ground station are large with respect to the wavelength. The antenna for pilot signal generation does not need to have large aperture in a practical SSPS system; and as a result, the ground station can be modeled as a point in Fig.14 as far as pilot signal is concerned. Nevertheless in order to collect wireless power efficiently, the ground station must employ a large antenna array with dimension on the order of $(\text{km})^2$. Thus as far as wireless power is concerned, the satellite and the ground station stay in each other's near-zone as well.

The scheme illustrated in Fig. 12 is usually termed "retro-directive beamforming" in Ref. [32]. As discussed in Section 0, "retro-directive beamforming" is a special case of "retro-reflective beamforming" when the wireless power transmitter and wireless power receiver stay in each other's far-zone, or equivalently, when pilot signal propaga-

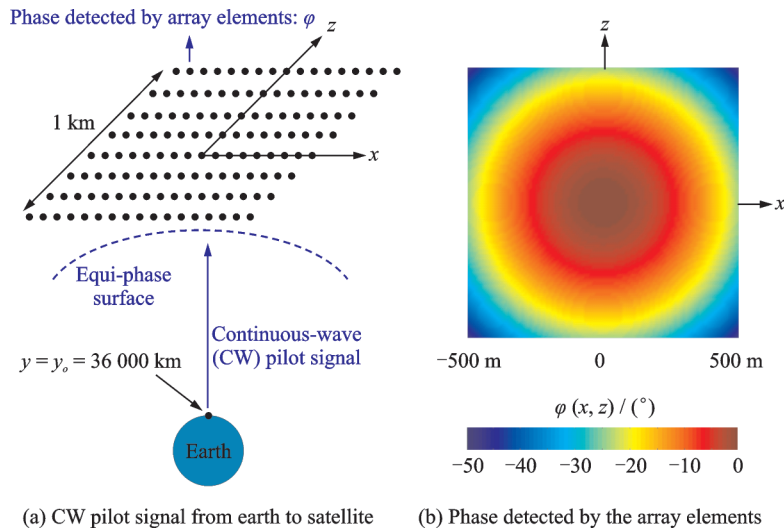


Fig.14 Phase detected by a 1 km by 1 km array when pilot signal is transmitted from the earth^[38]

tion and wireless power propagation could be characterized by plane waves with explicit propagation directions. Since the satellite and the earth are not in each other's far-zone in SSPS application (as evidenced by Fig.14), we find it more appropriate to use "retro-reflective beamforming" as the name of the scheme in Fig.12.

In the rest of this section, a preliminary experimental system is presented to demonstrate the retro-reflective beamforming technique for wireless power transmission in SSPS^[39].

The experimental setup is shown by a photo in Fig.15. A wireless power transmitter and a wireless power receiver are separated by 3 m approximately in space. The wireless power receiver emulates a ground station. It consists of four parts: a pilot signal generator, a pilot signal transmitting antenna, a wireless power receiving antenna, and a power meter to detect the wireless power. The wireless power transmitter emulates a space solar satellite. It consists of three parts: two pilot signal receiving antennas, two wireless power transmitting antennas, and a retro-reflective beamforming circuit. The interaction between wireless power transmitter and wireless power receiver involves two steps. In the first step, continuous-wave pilot signal at 2.9 GHz is broadcasted from the wireless power receiver to the wireless power transmitter. In the second step, the wireless power transmitter delivers directive power beam carried by continuous-wave at 5.8 GHz to the

wireless power receiver, in reaction to the pilot signal. Following the frequency-division scheme of Ref.[36], the pilot signal propagation and wireless power propagation employ 2.9 GHz and 5.8 GHz carrier frequencies, respectively, such that they could be isolated from each other using regular band-pass-filters.

All the antennas in Fig.15 are implemented by microstrip antennas. The two wireless power transmitting antennas are identical to each other. Each is composed of an 8×8 array of rectangular patches. The 8×8 array is designed to have a narrow radiation beam toward its broadside direction with gain value of 20.6 dBi at 5.8 GHz. The two wireless power transmitting antennas jointly constructs a narrower beam, and the beam can be steered along x direction (specified in Fig.15). The wireless power transmitting antennas are designed according to the practical requirements of SSPS application. In order to generate a narrow beam toward the earth, the antenna array over the satellite must include a large number of antenna elements. It would be cost-prohibitive to control these antenna elements individually; rather, it would be more cost-effective to group them into sub-arrays. One 8×8 array in Fig.15 embodies one sub-array of SSPS application. The feed network within one sub-array is fixed, and sub-arrays are excited by individual circuits in order to steer the wireless power beam. Obviously, the more elements each sub-array has, the lower the sat-

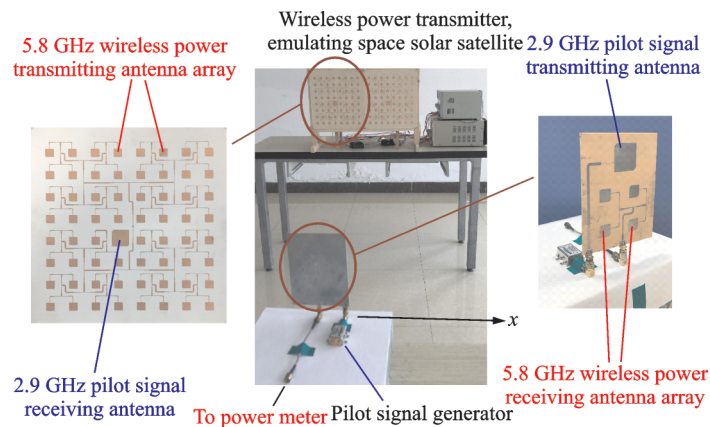


Fig.15 Setup of an experimental demonstration of wireless power transmission for SSPS application

ellite's cost and complexity would be. However, if a sub-array includes too many elements, each sub-array's radiation beam would be too narrow, which limits the range of beam steering. In an SSPS system, the size of sub-array must be optimized by taking various practical factors into account. The two pilot signal receiving antennas are located at the center of the two wireless power transmitting antennas, respectively, each consisting of one patch. The resonant frequency of the two pilot signal receiving antennas is 2.9 GHz, and as a result, they are physically larger than the 5.8 GHz patches. The two wireless power transmitting antennas have left-hand circular polarization at 5.8 GHz, and the two pilot signal receiving antennas have right-hand circular polarization at 2.9 GHz. The orthogonality between the two polarizations provides additional isolation between pilot signal propagation and wireless power propagation. Correspondingly at the wireless power receiver, there are a 2.9 GHz pilot signal transmitting antenna and a 5.8 GHz wireless power receiving antenna. The wireless power receiving antenna, including an array of four microstrip patches, has broadside gain value of 9 dBi at 5.8 GHz.

The pilot signal generator (highlighted in Fig. 15) generates 2.9 GHz pilot signal. The pilot signal is transmitted from the wireless power receiver and received by the wireless power transmitter. The functionality of the retro-reflective beamforming circuit (located behind the two wireless power transmitting antennas and not visible in Fig. 15) is to guarantee that a wireless power beam would be con-

structed toward the wireless power receiver in reaction to the pilot signal. The wireless power received by the wireless power receiver is detected by a power meter.

Some experimental results are plotted in Fig. 16. In the experiments, the wireless power transmitter is stationary, and the wireless power receiver moves along x axis specified in Fig. 15. " $x = 0$ " denotes the location right in front of the wireless power transmitter. The distance between the wireless power transmitter and " $x = 0$ " location is 3 m. The power transmitted by each wireless power transmitting antenna is approximately 10 dBm. In Fig. 16, wireless power data measured by the power meter in three experiments, termed Experiment A, Experiment B, and Experiment C, respectively, are plotted, as elaborated one by one next.

Experiment A The retro-reflective beamforming circuit is deactivated. The two wireless power transmitting antennas are excited with equal amplitude (10 dBm each) and equal phase. The wireless power receiver changes its location along x axis, and the power data measured by the power meter at various x locations are recorded and plotted.

Experiment B On the basis of Experiment A, a phase shifter is applied to adjust the difference between the two excitation phases from 0 to 360°. The wireless power receiver changes its location along x axis. At each location, the phase shifter is adjusted until the power received by the power meter reaches the maximum value. The maximum power data associated with various x locations are recorded and

plotted.

Experiment C Experiment B is conducted when the receiver is at “ $x = 0$ ” location. Afterwards, the retro-reflective beamforming circuit is employed, and the wireless power receiver changes its location along x axis. The power data measured by the power meter at various x locations are recorded and plotted.

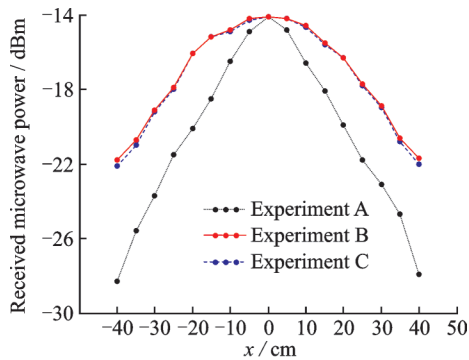


Fig.16 Measurement data of received wireless power in the setup of Fig.15^[39]

Among the three experiments above, Experiment C demonstrates the performance of retro-reflective beamforming, whereas Experiment A and Experiment B provide benchmark data. In Experiment A, the wireless power transmitter is not reconfigurable. Apparently, the curve associated with Experiment A in Fig.16 exhibits a wireless power beam centered at “ $x = 0$ ”, and the power level drops quickly when x deviates from 0. In Experiment B, the wireless power beam is reconfigured “manually” when the wireless power receiver’s location changes. It should be noted that Experiment B reveals the optimal performance of the wireless power transmitter. When the wireless power receiver’s location deviates from “ $x = 0$ ” by less than 15 cm, the wireless power beam tracks the wireless power receiver’s location with the fluctuation of received wireless power level smaller than 1 dB. The received wireless power level drops drastically when $|x| > 15$ cm, because the radiation beam of each individual wireless power transmitting antenna could not cover $|x| > 15$ cm. In Experiment C, the wireless power

transmitter is calibrated by the “ $x = 0$ ” location, and afterwards, the wireless power beam is capable of keeping track of the wireless power receiver’s location “automatically.” The Experiment C curve matches the Experiment B curve very well in Fig.16. It means that the proposed retro-reflective beamforming technique offers the close-to-optimal performance.

There are two wireless power transmitting antennas in the setup of Fig.15. More wireless power transmitting antennas could be incorporated straightforwardly. In Ref.[40], 2×2 wireless power transmitting antennas are included in a wireless power transmitter, and consequently, the wireless power transmitter is capable of steering wireless power beam along two dimensions.

3 Retro-reflective Beamforming Technique for Wireless Charging in Fully-Enclosed Space

Wireless charging pads are commercially available for the purpose of charging cell phones; one of the commercial products is shown in Fig.17(a). The underlying technique of wireless charging pads is inductive coupling^[41]. Since the inductive coupling technique relies on non-radiative magnetic field, cell phones must be physically placed on the pad in order to be charged efficiently. In other words, a wireless charging pad (as shown in Fig.17(a)) only takes advantage of certain two-dimensional surface. Apparently, a scheme that employs three-dimensional (in contrast to two-dimensional) space ought to offer higher charging capacity, which motivates the configuration in Fig.17(b). In the scheme illustrated in Fig.17(b), multiple electronic devices are deployed within a three-dimensional region and get charged simultaneously^[41]. The charging region is enclosed by a box with conducting walls, due to two concerns. First, the power level associated with wireless power transmission inside the box fully enclosed by conducting walls is not limited by regulations estab-

lished for human safety and/or electromagnetic compatibility^[24-26]. Second, since the conducting walls confine wireless power inside the box, high wireless power transmission efficiency (greater than 80%, for instance) is possible in the box. Basically, the scheme illustrated in Fig. 17(b) resembles a microwave oven. It is not a straightforward extension from the commercially-available wireless charging pads. Because wireless charging pads intend to minimize radiative fields, their operating frequencies are typically below 1 MHz^[42]. As far as the scheme in Fig. 17(b) is concerned, 1 MHz is a very low frequency, and the enclosed box behaves as a large capacitive load to the wireless power transmitter. In order to achieve conjugate matching, the wireless

power transmitter must incorporate a large inductance to neutralize the capacitive load. Fabricating a large inductor with accurate inductance value and high quality factor is well known to be a difficult task. Therefore in the scheme illustrated in Fig. 17(b), it is more optimal to upgrade the operating frequency to be close to the natural resonant frequencies of the enclosed box (typically higher than 100 MHz)^[43]. The box dedicated to wireless power transmission could be as large as a living room^[44-45]. Wireless power transmission in fully-enclosed space also has applications in many special practical environments with conducting enclosure, such as spacecrafts^[46], engine compartments^[47-48], greenhouses^[49], and medical experiments^[50-52].

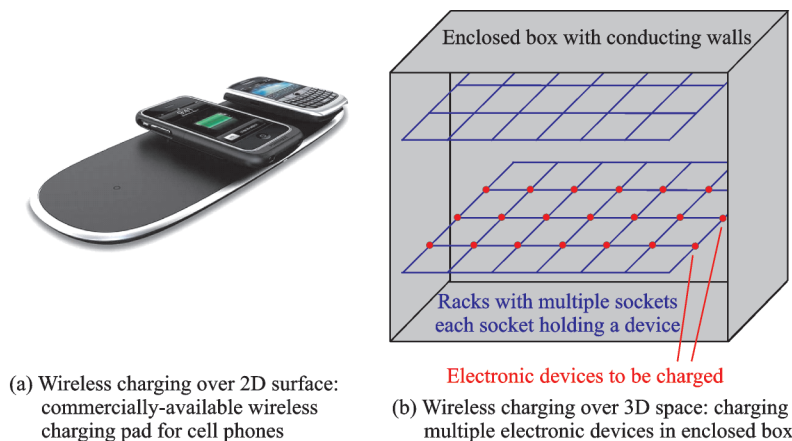


Fig.17 Wireless charging over two-dimensional surface versus wireless charging over 3D space

In fully-enclosed space, the conducting walls enforce the electromagnetic field to exhibit strong standing wave pattern. Consequently, the efficiency of wireless power transmission is very sensitive to spatial locations. Though the wireless power transmission efficiency could approach 100% in certain scenarios^[46], a wireless power receiver would receive little power if it resides at the “dark spots” of standing wave pattern. If a wireless power receiver is not stationary inside the box or if a wireless power receiver’s location is unknown to the wireless power transmitter, the standing wave pattern must be re-configured in real time to avoid dark spots from the wireless power receiver’s location. As a matter of fact, the dark spots issue occurs in microwave oven

too, and it is resolved by either rotating the food or stirring the field distribution. In Ref.[53], mechanical stirring is applied to perturb the standing wave patterns and in turn improve wireless power transmission efficiency in the statistical sense. The research in Refs.[54-55] takes advantage of multiple frequencies/modes to relieve the dark spots’ impact. Recently, we propose a parasitic array architecture to reconfigure wireless power transmission in fully-enclosed space^[56-57]. In a parasitic array, only one antenna element, termed as “driver element”, is excited by a power source. The other antenna elements in the parasitic array, termed as “parasitic elements”, are terminated by purely-reactive loads. After the source’s power is radiated by

the driver element, certain portion of the power is coupled to the parasitic elements. Further because the parasitic elements are terminated by purely-reactive loads, the coupled power is re-radiated into the fully-enclosed space. The total electromagnetic field in the fully-enclosed space is the sum of direct radiation from the driver element and re-radiation from the parasitic elements. If the reactive loads are tunable, the re-radiation's phase would be altered and the total field in the fully-enclosed space would be reconfigured. Parasitic array may be a more appealing resolution to reconfigure wireless power transmission than Refs. [53-55] in certain applications, as it does not call for mechanical reconfiguration or wideband antennas/circuits. A similar scheme is proposed in Ref. [58], in which the parasitic elements are termed "matching probes". Parasitic array is not a new concept. As a matter of fact, the classic Yagi-Uda antenna is a parasitic array. In a Yagi-Uda antenna, only one element of the array is connected to a source/excitation, and the other elements can be modeled as dipoles terminated by short^[37]. Some of our preliminary investigations of using parasitic array to reconfigure wireless power transmission in fully-enclosed space are presented in the following.

As illustrated by Fig.18, wireless power is tr-

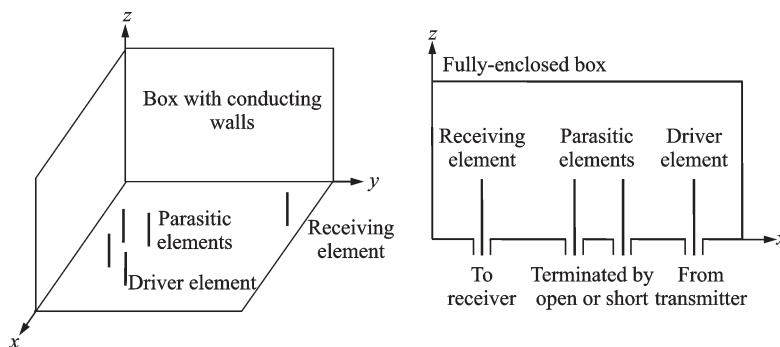


Fig.18 Depiction of using parasitic antenna array to reconfigure wireless power transmission in fully-enclosed space

In an experimental configuration illustrated by Fig. 20, there are one driver element located at ($x = 70$ cm, $y = 20$ cm) and nine parasitic elements. The nine parasitic elements are terminated by either short or open. Apparently, there are $2^9 = 512$ combinations of reconfigurability in total. The power transmission efficiency of all the combina-

nsmitted by one driver element with the aid of multiple parasitic elements in a rectangular box with conducting walls. The driver element and parasitic elements have fixed locations. Wireless power is received by one receiving element whose location is not fixed. The driver element, parasitic elements, and receiving element are monopoles oriented along z direction. The driver element and receiving element are connected to a transmitter and a receiver through co-axial connectors, respectively. The parasitic elements are terminated at $z = 0$ plane by either open or short. A photo of our experimental setup is shown in Fig.19. The box in the experiments is cubic with side length of 1 m and with its six walls made of aluminum. As a difference between Figs.18 and 19, z axis is downward in Fig.19, in order to facilitate routing the cables and adjusting the parasitic elements' termination. The driver element, parasitic elements, and receiving element are all made of copper wires with length of 17 cm. Scattering parameters with respect to standard $50\text{-}\Omega$ characteristic impedance are measured between the driver element (Port 1) and receiving element (Port 2) at 425 MHz by a network analyzer manufactured by Radasun Instruments with model number AV3620A.

tions is measured, and the maximum power transmission efficiency is recorded. In the results plotted in Fig.21, the receiving element changes its location in the shaded region of Fig.20. Measurement data of three scenarios are presented in Fig.21: "0 parasitic" "6 parasitic" and "9 parasitic". In the "0 parasitic" scenario, there are no parasitic elements. In the

as the retro-reflective beamforming schemes in Section 1 and Section 2 fundamentally, as it takes advantage of two-way propagation: pilot signal propagation in the first step and wireless power propagation in the second step. The primary difference be-

tween this section and the previous two sections is that, the retro-reflective beamforming schemes in Section 1 and Section 2 rely on phased array, whereas the retro-reflective beamforming scheme in this section relies on parasitic array.

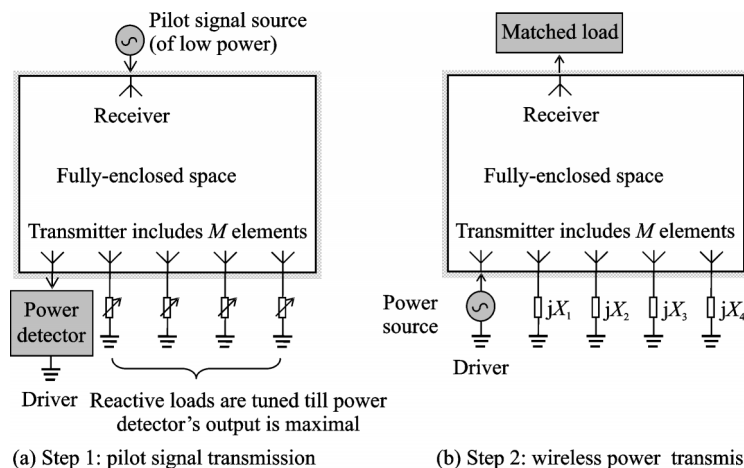


Fig.22 Retro-reflective beamforming scheme based on parasitic array for wireless power transmission in fully-enclosed space

4 Conclusions

In this paper, our recent research endeavors on retro-reflective beamforming technique are reviewed in the context of three applications of wireless power transmission: (1) wireless charging for low-power mobile/portable electronic devices, (2) SSPS application, and (3) wireless charging in fully-enclosed space. Preliminary experimental results demonstrate that, retro-reflective beamforming technique is capable of focusing microwave power onto a wireless power receiver's location via analyzing the pilot signal broadcasted by the wireless power receiver. We are currently conducting more in-depth research on retro-reflective beamforming technique as well as applying it in practice.

References

- [1] GARNICA J, CHINGA R A, Lin J. Wireless power transmission: From far field to near field [J]. Proceedings of the IEEE, 2013, 101(6): 1321-1331.
- [2] BROWN W C. The history of power transmission by radio waves [J]. IEEE Transactions on Microwave Theory and Techniques, 1984, 32(9): 1230-1242.
- [3] STEINSIEK F, WEBER K H, FOTH W P, et al. Wireless power transmission experiment using an air-
- ship as relay system and a moveable rover as ground target for later planetary exploration missions [C]// The 8th ESA Workshop on Advanced Space Technologies for Robotics and Automation. Noordwijk, The Netherlands: [s.n.], 2004: 10.2514/6.IAC-03-R.3.06.
- [4] KIM S M. Wireless optical energy transmission using optical beamforming [J]. Optical Engineering, 2013, 52(4): 043205.
- [5] BROWN W C. Experimental airborne microwave supported platform [R]. Raytheon CO Burlington MA Spencer Lab Report, 1965.
- [6] DICKINSON R M. Evaluation of a microwave high-power reception-conversion array for wireless power transmission [R]. Jet Propulsion Lab Tech Memo 33-741, 1975.
- [7] DICKINSON R M, BROWN W C. Radiated microwave power transmission system efficiency measurements [R]. Jet Propulsion Lab Tech Memo 33-727, 1975.
- [8] SCHLESACK J, ALDEN A, OHNO T. SHARP rec-tenna and low altitude flight trials [C]//Global Telecommunications Conference. New Orleans, LA: [s.n.], 1985.
- [9] FUJINO Y, ITO T, FUJITA M, et al. A rectenna for MILAX [C]//The 1st Annual Wireless Power Transmission Conference. San Antonio, TX: [s.n.], 1993.

- [10] KAYA N, KOJIMA H, MATSUMOTO H, et al. ISY-METS rocket experiment for microwave energy transmission[J]. *Acta Astronautica*, 1994, 34: 43-46.
- [11] CELESTE A, JEANTYA P, PIGNOLET G. Case study in reunion island [J]. *Acta Astronautica*, 2004, 54(4): 253-258.
- [12] MASCARENAS D L, FLYNN E B, TODD M D, et al. Experimental studies of using wireless energy transmission for powering embedded sensor nodes [J]. *Journal of Sound and Vibration*, 2010, 329 (12) : 2421-2433.
- [13] WANG X, LU M. Wireless power transfer-fundamentals and technologies: Microwave power transmission based on retro-reflective beamforming[M]. Rijeka, Croatia: InTech, 2016: 89-108.
- [14] HENTY B E, STANCIL D D. Multipath-enabled super-resolution for RF and microwave communication using phase-conjugate arrays[J]. *Physical Review Letters*, 2004, 93: 243904.
- [15] DE ROSNY J, FINK M. Focusing properties of near-field time reversal[J]. *Physical Review A—Atomic, Molecular, and Optical Physics*, 2007, 76 (6): 065801.
- [16] LEROSEY G, DE ROSNY J, TOURIN A, et al. Focusing beyond the diffraction limit with far-field time reversal[J]. *Science*, 2007, 315: 1120-1122.
- [17] CHIU L, YUM T Y, CHANG W S, et al. Retrodirective array for RFID and microwave tracking beacon applications[J]. *Microwave and Optical Technology Letters*, 2006, 48(2): 409-411.
- [18] MIYAMOTO R Y, ITOH T. Retrodirective arrays for wireless communications[J]. *Microwave Magazine*, 2002, 3: 71-79.
- [19] VITAZ J A, BUERKLE A M, SARABANDI K. Tracking of metallic objects using a retro-reflective array at 26 GHz[J]. *IEEE Transactions on Antennas and Propagation*, 2010, 58(11): 3539-3544.
- [20] WANG X, RUAN B, LU M. Retro-directive beamforming versus retro-reflective beamforming with applications in wireless power transmission[J]. *Progress in Electromagnetics Research*, 2016, 157: 79-91.
- [21] TSENG W J, CHUNG S J, CHANG K. A planar Van Atta array reflector with retrodirectivity in both E-plane and H-plane[J]. *IEEE Transactions on Antennas and Propagation*, 2000, 48(2): 173-175.
- [22] PON C. Retrodirective array using the heterodyne technique[J]. *IEEE Transactions on Antennas and Propagation*, 1964, 12: 176-180.
- [23] BUCHANAN N B, FUSCO V F. Triple mode PLL antenna array[C]//International Microwave Symposium. Fort Worth, TX: IEEE, 2004: 10.1109/MWSYM.2004.1338915.
- [24] IEEE. Safety levels with respect to human exposure to radio frequency electromagnetic fields, 3 kHz to 300 GHz[S]. IEEE C95.1—1991. Piscataway, NJ: IEEE, 2005.
- [25] Federal Communications Commission. Rules & regulations for title 47 [EB/OL]. (2019-07-05). <http://transition.fcc.gov/oet/info/rules/>.
- [26] ICNIRP. Frequencies and applications[EB/OL]. (2019-07-05). <http://www.icnirp.de/>.
- [27] VISSER H J, VULLERS R J M. RF energy harvesting and transport for wireless sensor network applications: Principles and requirements[J]. *Proceedings of the IEEE*, 2013, 101(6): 1410-1423.
- [28] ZHAI H, PAN H K, LU M. A practical wireless charging system based on ultra-wideband retro-reflective beamforming[C]//IEEE Antennas and Propagation Symposium. Toronto, Canada: IEEE, 2010: 10.1109/APS.2010.5561113.
- [29] WANG X, SHA S, HE J, et al. Wireless power delivery to low-power mobile devices based on retro-reflective beamforming[J]. *IEEE Antennas and Wireless Propagation Letters*, 2014, 13: 919-922.
- [30] HE J, WANG X, GUO L, et al. A distributed retro-reflective beamformer for wireless power transmission[J]. *Microwave and Optical Technology Letters*, 2015, 57(8): 1873-1876.
- [31] GLASER P. Power from the sun: Its future[J]. *Science*, 1968, 162(3856): 857-861.
- [32] STRASSNER B, CHANG K. Microwave power transmission: Historical milestones and system components[J]. *Proceedings of the IEEE*, 2013, 101(6) : 1379-1396.
- [33] Caltech. Space solar power project[EB/OL]. (2019-07-05). <https://www.spacesolar.caltech.edu/>.
- [34] SASAKI S, TANAKA K, MAKI K-I. Microwave power transmission technologies for solar power satellites [J]. *Proceedings of the IEEE*, 2013, 101(6) : 1438-1447.
- [35] Mitsubishi Heavy Industries, Ltd. MHI successfully completes ground demonstration testing of wireless power transmission technology for SSPS—Expanding the potential for new industrial applications[EB/OL]. [2015-03-12] (2019-07-05). <https://www.mhi.com/news/story/1503121879.html>.
- [36] HSIEH L H, STRASSNER B H, KOKEL S J, et al. Development of a retrodirective wireless micro-

- wave power transmission system[C]//IEEE International Symposium on Antennas and Propagation. Columbus, OH: IEEE, 2003; 10.1109/APS.2003.1219259.
- [37] BALANIS C A. Antenna theory: Analysis and design[M]. 3rd ed. New York: Wiley-Interscience, 2005.
- [38] WANG X, HOU X, WANG L, et al. Employing phase-conjugation antenna array to beam microwave power from satellite to earth[C]//IEEE International Conference on Wireless for Space and Extreme Environments. Orlando, FL: IEEE, 2015; 10.1109/WISSEE.2015.7393093.
- [39] CHENG H, CAO X, WANG X, et al. A retro-reflective beamforming scheme based on heterodyne technique for wireless power transmission[C]//International Applied Computational Electromagnetics Society (ACES) Symposium. Beijing, China: ACES, 2018; 10.1109/APS.2015.7304592.
- [40] CAO X, CHENG H, WANG X, et al. Retro-reflective beamforming for wireless power transmission based on harmonic mixing scheme[C]//The 11th International Conference on Microwave and Millimeter Wave Technology. Guangzhou, China: [s.n.], 2019.
- [41] CHEN C, WANG X, LU M. Wireless charging to multiple electronic devices simultaneously in enclosed box[C]//Asia-Pacific International Symposium on Electromagnetic Compatibility. Shenzhen, China: [s.n.], 2016; 10.1109/APEMC.2016.7522884.
- [42] Wireless Power Consortium. Product database[EB/OL]. (2019-07-05). <http://www.wirelesspowerconsortium.com/technology/low-frequency-non-radiative-power-transfer.html>.
- [43] CHABALKO M J, SAMPLE A P. Resonant cavity mode enabled wireless power transfer[J]. Applied Physics Letters, 2014, 105(24): 243902.
- [44] CHABALKO M J, SHAHMOHAMMADI M, SAMPLE A P. Quasistatic cavity resonance for ubiquitous wireless power transfer[J]. PLoS ONE, 2017, 12(2): e0169045.
- [45] SASATANI T, YANG J, CHABALKO M J, et al. Room-wide wireless charging and load-modulation communication via quasistatic cavity resonance[J]. Proceedings of the ACM on Interactive, Mobile, Wearable and Ubiquitous Technologies, 2018, 2(4): 1-23.
- [46] WU J, LIANG J, WANG X, et al. Feasibility study of efficient wireless power transmission in satellite interior[J]. Microwave and Optical Technology Letters, 2016, 58(10): 2518-2522.
- [47] GOTO H, SHINOHARA N, MITANI T, et al. Study on microwave power transfer to sensors in car engine compartment[C]//IEEE Wireless Power Transfer Conference. Jeju, Korea: IEEE, 2014; 10.1109/WPT.2014.6839588.
- [48] TAKANO I, FURUSU D, WATANABE Y, et al. Study on cavity resonator wireless power transfer to sensors in an enclosed space with scatterers[C]//IEEE MTT-S International Conference on Microwaves for Intelligent Mobility. Nagoya, Japan: IEEE, 2017; 10.1109/ICMIM.2017.7918861.
- [49] TAKANO I, FURUSU D, WATANABE Y, et al. Cavity resonator wireless power transfer in an enclosed space with scatterers utilizing metal mesh[J]. IEICE Transactions on Electronics, 2017, E100-C (10) : 841-849.
- [50] MONTGOMERY K L, YEH A J, HO J S, et al. Wirelessly powered, fully internal optogenetics for brain, spinal and peripheral circuits in mice[J]. Nature Methods, 2015, 12(10): 969-974.
- [51] MEI H, THACKSTON K A, BERCIH R A, et al. Cavity resonator wireless power transfer system for freely moving animal experiments[J]. IEEE Transactions on Biomedical Engineering, 2017, 64 (4) : 775-785.
- [52] SHIN G, GOMEZ A M, AL-HASANI R, et al. Flexible near-field wireless optoelectronics as subdermal implants for broad applications in optogenetics[J]. Neuron, 2017, 93(3): 509-521.
- [53] KORHUMMEL S, ROSE N A, POPOVIC Z. Over-moded cavity for multiple-electronic-device wireless charging[J]. IEEE Transactions on Microwave Theory and Techniques, 2014, 62(4): 1074-1079.
- [54] CHABALKO M J, SAMPLE A P. Three-dimensional charging via multi-mode resonant cavity enabled wireless power transfer[J]. IEEE Transactions on Power Electronics, 2015, 30(11): 6163-6173.
- [55] SASATANI T, CHABALKO M J, KAWAHARA Y, et al. Multimode quasistatic cavity resonators for wireless power transfer[J]. IEEE Antennas and Wireless Propagation Letters, 2017, 16: 2746-2749.
- [56] WANG X, CHEN C, LU M. A reconfigurable scheme of wireless power transmission in fully-enclosed box[C]//The 18th Annual International Conference on Industrial Technology. Toronto, Canada: [s.n.], 2017; 10.1109/ICIT.2017.7915559.
- [57] WANG X, CHEN C, WONG H, et al. A reconfigu-

nable scheme of wireless power transmission in fully enclosed environments [J]. *IEEE Antennas and Wireless Propagation Letters*, 2017, 16: 2959-2962.

- [58] NIMURA S, FURUSU D, TAKANO I, et al. Improvement in transmission efficiency for cavity resonance enabled wireless power transfer by handling cavity impedance [C]//*Asia-Pacific Microwave Conference*. Kyoto, Japan:[s.n.], 2018.

Acknowledgements This work was supported in part by the National Natural Science Foundations of China (Nos. 61871220, 61471195, 61628106), and the United States National Science Foundation (Nos. ECCS 1303142, ECCS 1503600).

Authors Prof. WANG Xin received the Ph.D. degree in electrical and computer engineering from Purdue University, West Lafayette, IN, USA in 2009. He is currently an associate professor at the College of Electronic and Information En-

gineering, Nanjing University of Aeronautics and Astronautics, China. His research interest includes wireless power transmission, reconfigurable antennas, and RF circuits.

Prof. LU Mingyu received the Ph.D. degree in electrical engineering from the University of Illinois, Urbana-Champaign, IL, USA in 2002. He is currently a full professor at the Department of Electrical and Computer Engineering, West Virginia University Institute of Technology, USA. His research interest includes wireless power transmission, radar systems, microwave remote sensing, antenna design, and computational electromagnetics.

Author contributions Prof. LU Mingyu's contributions are largely on the theoretical analysis, and Prof. WANG Xin's contributions are primarily on the experimental verification.

Competing interests The authors declare no competing interests.

(Production Editor: Zhang Huangqun)